Journal of Zhejiang University-SCIENCE C (Computers & Electronics)
ISSN 1869-1951 (Print); ISSN 1869-196X (Online)
www.zju.edu.cn/jzus; www.springerlink.com
E-mail: jzus@zju.edu.cn

Cranio-maxillofacial surgery simulation based on pre-specified target face configurations*

Sheng-zheng WANG†[1,2], Jie YANG[1], James C. GEE[3]

([1]*Institute of Image Processing & Pattern Recognition, Shanghai Jiao Tong University, Shanghai 200240, China*)

([2]*Merchant Marine College, Shanghai Maritime University, Shanghai 200235, China*)

([3]*Department of Radiology, University of Pennsylvania, Philadelphia 19104, PA, USA*)

†E-mail: szwang.smu@gmail.com

Received June 12, 2009; Revision accepted Oct. 26, 2009; Crosschecked May 19, 2010

Abstract: This paper presents a novel method for assisting surgeons in automatically computing an optimal surgical plan by directly specifying the desired correction to a facial outline. First, the desired facial appearance is designed using a 3D sculpturing tool, while the cut regions of the skull are defined based on facial anatomy. Then, the deformation of the face meshes is performed using an improved biomechanical model in which virtual external forces are driven by the displacements corresponding to the differences of node coordinates between the original and specified face meshes, and free nodes and fixed nodes are defined in terms of the contact surfaces between the soft tissues and the bones within the cut regions. Finally, the shape of the contact surfaces is updated following the deformation of the soft tissues. After registering the deformable contact surfaces and the cut surfaces, the final positions of the cut bones are estimated. Evaluation of preliminary experimental results quantitatively shows the effectiveness of the proposed approach.

Key words: Surgical planning, Biomechanical modeling, Soft tissue deformation, Plastic surgery
doi:10.1631/jzus.C0910349 **Document code:** A **CLC number:** TP319

1 Introduction

Plastic surgery is one of the most popular cosmetic procedures. The goal is to improve the cranio-maxillofacial aesthetically, by harmonizing it with other facial features; thus, the capacity to set up and design the optimal surgery schemes within a computer-assisted surgical (CAS) planning system presents a critical need for surgeons. In the past, many methods have been proposed, in the form of CAS planning systems, for performing bone-related pre-operative planning and deformation simulation of soft tissues. The former includes osteotomy simulation, and tools for virtual distraction and evaluation (Everett *et al*., 2000; Schutyser *et al*., 2000). For deformation simulation of soft tissues, earlier work in this field mainly focused on animation based on masses and springs (Lee *et al*., 1995), which was widely used in facial animation. These applications had a different emphasis from those applied in surgical simulators. The intention of the animation was to realistically mimic facial expressions, not to simulate the accurate physical behavior of human soft tissues. Afterwards, several facial soft tissue models based on finite element modeling were developed (Keeve *et al*., 1996; Koch *et al*., 1996). Unfortunately, the features of living tissues were not taken into account in these models, and thus the deformations of the soft tissues were unrealistic. Consequently, some research has focused on the biomechanical modeling of soft tissues (Zachow *et al*., 2000; Gladilin *et al*., 2001). Moreover, non-linear and anisotropic deformable models were proposed to enhance the accuracy of the deformations of the soft tissues (Picinbono *et*

* Project supported by the Academic Discipline Project (No. S30602) and the Shanghai Science Foundation of China (No. 08ZR1409300)

al., 2001; 2003). In addition, Zachow *et al*. (2006) presented a general procedure to model, plan, and simulate the plastic surgery in a CAS, which allows for pre-operative assessment of different therapeutic strategies. Furthermore, much work has been performed to quantitatively and qualitatively evaluate the effectiveness of the deformable models of the soft issues (Zachow *et al*., 2004; Westermark *et al*., 2005; Mollemans *et al*., 2007).

Nevertheless, the methods remain limited to the prediction of soft tissue deformation. The bone-related planning that affects the desired tissue deformation must still be developed by the surgeon. This process is both tedious (one must iterate through multiple skull-remodeling plans before converging on a suitable solution) and challenging (the precise face configuration sought after may be difficult to obtain with this approach). A superior strategy would first allow the desired facial outline to be specified, and then automatically determine the appropriate surgical plan that precisely yields the post-operative facial appearance of interest. This approach is addressed in this work, and is also effectively the inverse problem in predicting soft tissue deformation. The implementation employs an improved biomechanical model for the face to enhance tissue behavior in the simulation. Specifically, mixed element modeling is developed to allow skin and soft tissues to be discretized with different finite element types and assigned with unique material properties. The approach automatically generates the new positions of cut bones with which surgical plans can be optimized to obtain the final facial configuration.

2 Materials and methods

2.1 Material properties

Soft tissues generally exhibit anisotropic, non-homogeneous, non-linear, and plastic-viscoelastic material properties (Fung, 1993). In this paper, to simplify finite element modeling, the non-linear mechanical behaviors of the bulk soft tissues are defined through a hyper-elastic model. The investigation of the hyper-elastic models was conducted in Chabanas *et al.* (2004), Natali *et al.* (2006), Sokhanvar *et al.* (2008), and Wang and Yang (2009). In addition, Wang and Yang (2010) evaluated the effectiveness of the hyper-elastic models, and investigated the choice of the strain energy functions and material parameters. The general hyper-elastic model is summarized as follows.

A hyper-elastic large strain model generally can be represented by a strain energy density function,

$$W = W(\boldsymbol{C}), \tag{1}$$

where $\boldsymbol{C}$ is the right Cauchy-Green tensor.

To choose an appropriate strain energy density function, the facial soft tissue is assumed to be nearly incompressible, homogeneous, and isotropic elastic material, and thus the two-term Mooney-Rivlin (M-R) equation can be used to express the strain energy function:

$$W(I_1, I_2) = C_{10}(I_1 - 3) + C_{01}(I_2 - 3), \tag{2}$$

where C_{10} and C_{01} are material constants, and I_1 and I_2 are the first and second deviatoric strain invariants of $\boldsymbol{C}$, respectively.

The experimental stress-strain data is used in the estimation of the material constants. As shown in Fig. 1, the coarse experimental data of the skin, muscles, and fat can be found in Fung (1993) and Kvistedal and Nielsen (2004). Fig. 2 shows the approximate results of the different soft tissues using the least square curve-fitting procedure. The actual values employed in the hyper-elastic model associated with the non-linear mechanical definition of the soft tissues were estimated and presented in Table 1.

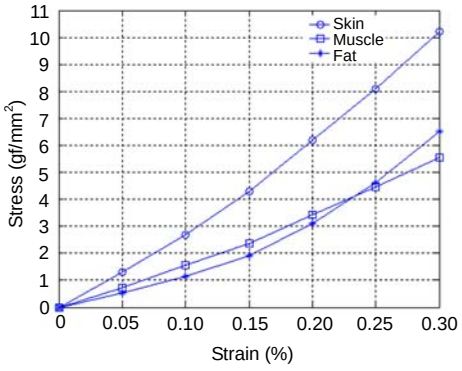

Fig. 1 Strain-stress relationship of the soft tissues

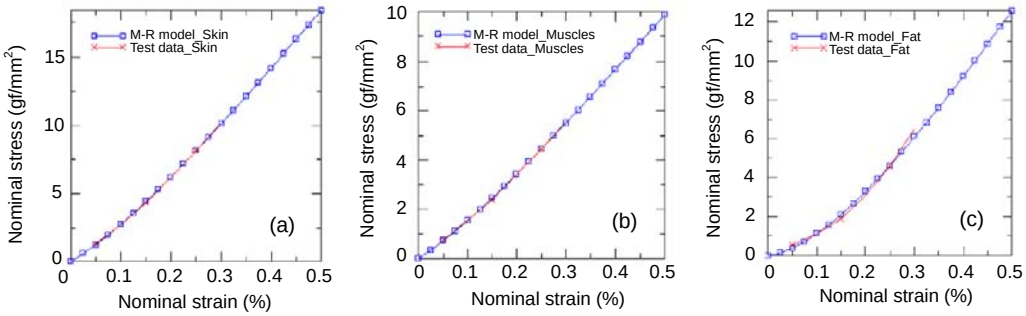

Fig. 2 Material properties evaluation results

(a) Fitted curve of the Mooney-Rivlin (M-R) material model for skin; (b) Fitted curve for muscles; (c) Fitted curve for fat

Table 1 Hyper-elastic material parameters of the soft tissues for the Mooney-Rivlin model

Soft tissue	D_1	C_{10} (gf/mm^2)	C_{01} (gf/mm^2)
Skin	0.49	18.9834	−15.4072
Muscle	0.30	9.8454	−7.7433
Fat	0.49	16.6131	−16.0127

D_1 determines compressibility; C_{10} and C_{01} are constants to control stiffness

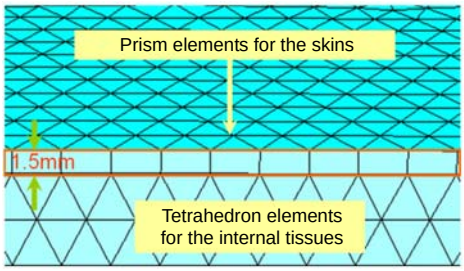

Fig. 3 Geometric structures of the mixed elements

2.2 Biomechanical modeling of the soft tissues

In conventional deformable models, all soft tissues are represented by a unique geometric element type, which could not exactly model the anatomic structures of the soft tissues since the soft tissues have complex geometric structures and mechanical properties. Hence, most of the existing models lack accuracy in simulating the deformation of the facial soft tissues.

To improve the deformable model of the soft tissues, we introduce the mixed element modeling to simulate the facial soft tissues (Wang and Yang, 2010; Wang *et al*., 2010). As shown in Fig. 3, the skin tissues are discretized into prism elements and the internal tissues (muscles and fat) into tetrahedron elements.

For the mixed element modeling, the principal task is to discretize the skins and the internal soft tissues using the prism elements and the tetrahedron elements, respectively. During this process, the skin and skull surfaces first are reconstructed from computed tomography (CT) datasets using the marching cubes algorithm and are optimized with some mesh algorithms (Keeve *et al.*, 1997; Paiva *et al.*, 2006). Then, the external surfaces of the internal tissues are obtained by moving the vertices of the skin surface along the vertex normal by an amount of ζ in negative direction (ζ is the assumed thickness of the skin). In general, ζ averages 1.5 mm. Thus, a geometric model based on the mixed elements is built.

As shown in Fig. 3, the skin tissues are discretized into a number of prism elements, and the internal tissues are discretized into a number of tetrahedron elements.

In biomechanical modeling, another task is to design reasonable shape functions which affect the model accuracy and the computational efficiency. Generally speaking, applying high-order shape functions can enhance the accuracy, but it increases the computational burden. Therefore, the C^1-continuous shape functions are used at the facial surface and the C^0-continuous shape functions in the interior elements so as to balance the accuracy and the efficiency, which meets both the need for rendering smooth surface and the demand to conform to the underlying physics. That is to say, the prism elements are represented by the C^1-continuous shape functions and the tetrahedron elements are based on the C^0-continuous shape functions. However, the prism elements and the tetrahedron elements cannot be connected because of the discontinuousness of the number of degrees of

freedom between them. Therefore, the special transition shape functions are used to solve the discontinuity of the degrees of freedom between them using the special transition shape functions.

Both the tetrahedron elements and the prism elements are represented by linear shape functions, which reduce largely the total number of degrees of freedom of the system; thus, the linear shape functions of the tetrahedron elements are defined as

$$N_i(L) = L_i, \quad i = 1,2,3,4, \tag{3}$$

where L_i are the volume barycentric coordinates of the tetrahedral element.

Likewise, the linear shape functions of the prism elements are written as

$$\boldsymbol{N}^6(r,s,t,q) = [r(1-q), s(1-q), t(1-q), rq, sq, tq], \tag{4}$$

where r, s, and t are the barycentric coordinate parameters of the triangle surface, and q is the volumetric extension with q=0 at the top surface and q=1 at the bottom surface of the prism element.

In order to render the smooth surface of the skins, the C^1-continuous shape functions of the prism element are expected at the facial surface. Therefore, the novel shape functions are developed by extending the shape functions of the plate-bending element. As shown in Fig. 4, a plate-bending element is defined as

$$\boldsymbol{N}^{9*} = \boldsymbol{N}^9 + [j_{23}, j_{31}, j_{12}](\boldsymbol{Y} - \boldsymbol{Z}), \tag{5}$$

where j_{23}, j_{31}, and j_{12} are the correcting functions, $\boldsymbol{N}^9$ are the basic Hermite interpolation functions of a triangular element, $\boldsymbol{Y}$ is the average of the corresponding cross-boundary derivatives at the endpoints of each edge, and $\boldsymbol{Z}$ is the cross-boundary derivatives at the edge midpoints (refer to Wang *et al.* (2010) for details).

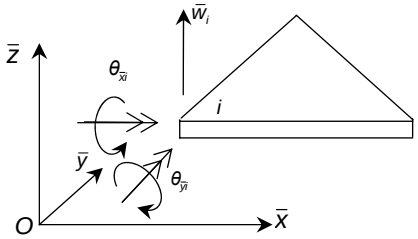

Fig. 4 A plate-bending element with three nodes

Hence, by Eqs. (4) and (5), the shape functions of the prism element can be extended as

$$\boldsymbol{N}^{12}(r,s,t,q) = \left[\boldsymbol{N}^{9*}(1-q), rq, sq, tq\right]. \tag{6}$$

Thus, the special transition shape functions featuring C^1-continuity at the facial surface and C^0-continuity at the internal elements are constructed (Fig. 5).

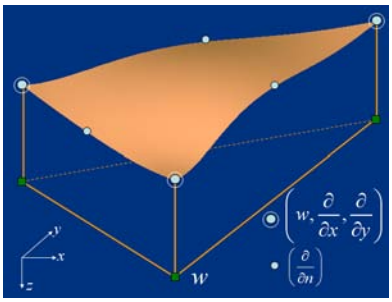

Fig. 5 Prism elements with the C^1-continuous surface at the top and C^0-continuity at the bottom plane

The interpolation functions of the mixed elements are defined as

$$u(\boldsymbol{x}) = \sum_{i=1}^{n} N_i \boldsymbol{u}_i, \tag{7}$$

where $\boldsymbol{x}$ is a given point of the current geometric configuration, $\boldsymbol{u}_i$ is the ith node's displacement, N_i (i=1, 2, …, n) are the shape functions, and n is the number of nodal points.

2.3 Simulation of soft tissue deformation

The simulation of the soft tissue deformation involves three tasks. The first task is to build a biomechanical model of the soft tissues based on the mixed-element modeling and hyper-elastic material relationship as described in Sections 2.1 and 2.2. The second task is to define the boundary conditions of the biomechanical model, and the final task is to solve the biomechanical mode.

In the second task, in order to solve for the bone displacements that would affect the desired facial appearance, the following boundary conditions are defined: the interface between the soft tissues contacting the cut bone surfaces is defined as Γ_n; the

remaining inner surface tissue nodes adjoining bone form the fixed boundary Γ_c; the displacements corresponding to the differences in nodal position between pre-specified and original facial meshes are used to specify the virtual external boundary Γ_e. The various surfaces over which different boundary conditions are specified can be seen in Fig. 6.

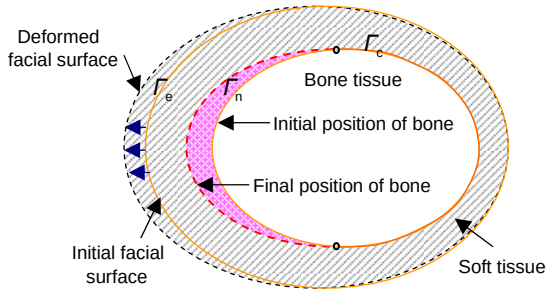

Fig. 6 Boundary value problem arising from the proposed craniofacial surgical planning approach

The traction force of the nodes of the facial surface is

$$\boldsymbol{f}_e = K_e\left(\left\|\boldsymbol{p}_{i0}-\boldsymbol{p}_{i1}\right\|-L_i^0\right)\frac{\boldsymbol{p}_{i0}-\boldsymbol{p}_{i1}}{\left\|\boldsymbol{p}_{i0}-\boldsymbol{p}_{i1}\right\|}, \tag{8}$$

where K_e is a penalty constant, L_i^0 is the rest length, and $\boldsymbol{p}_{i0}$ and $\boldsymbol{p}_{i1}$ represent the 3D coordinates of vertex i on the original and pre-specified meshes, respectively.

The virtual external force is therefore computed as follows:

$$\boldsymbol{F}_a^{\text{cont}} = \int_{\partial V^{(c)}} \boldsymbol{f}_e N_a \mathrm{d}a. \tag{9}$$

3 Results

All algorithms in this paper were performed on a workstation with a Dual-Core AMD Opteron CPU 3.0 GHz, with 4 GB of RAM, and an NVIDIA Quadro FX 5500 GPU.

A typical case of the plastic surgery was used to explain the simulation procedure of the surgical planning in Section 3.1. In addition, we analyze the errors from a different perspective in Section 3.2.

3.1 System implementation

For a mid-face plastic surgery, the objective is to correct the craniofacial dysostosis using the mid-face distraction osteotogenesis. The implementation consists of the following steps:

1. 3D mesh construction. The CT data of the patients can be first semi-automatically segmented using the ITK-SNAP tool (ITK-SNAP, 2009), and then the 3D surface mesh modes of the facial soft tissues and the bones are generated by applying the marching cubes algorithm. Finally, a mixed volumetric mesh model containing all the facial tissues is built as described in Section 2.2. The time for the mesh generation is more or less 3 min.

2. Pre-specification of the target facial profile. After reconstruction of the skull and the pre-operative facial surface, the surgeon can inspect these models in a 3D environment and imagine the patient's post-operative facial appearance. Based on the inspection of these models and the planning data, the skin-layer of the original 3D mesh on the mid-face is warped into its desired shape using a 3D sculpturing tool, as available, for example, with Maya 7.0 (Fig. 7).

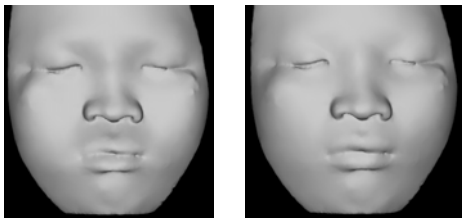

(a) (b)

Fig. 7 Pre-operative (a) and desired post-operative (b) faces

3. Osteotomies. After specifying a target face configuration, the next step is to define the cut regions of the bones. The bone cuts (osteotomies) must be done by a craniofacial surgeon since the osteotomies relate to the anatomy of the face and the validity of the soft tissue deformation. Therefore, the required cut surfaces are interactively generated by a surgeon following the anatomic structures and the target face configuration (Fig. 8a).

4. Boundary condition computation. After the definition of the cut regions, boundary conditions are computed. Virtual external forces for the finite element model are derived with respect to the measured

differences in node coordinates between the original and pre-specified facial meshes. The displacements of the skin-layer nodes are shown in Fig. 8b.

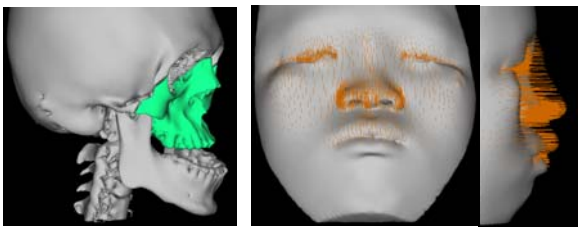

(a) (b)

Fig. 8 Definition of osteotomies (a) and displacements of the skin-layer nodes (b)

5. Simulation. The geometrical model and the boundary conditions serve as input to our simulator. The mixed-element biomechanical model described in Section 2 is used to model the facial soft tissue behavior and to estimate the new position of the inner soft tissue surface. The average simulation time is more or less 20 min.

6. Registration. To quantify the displacements of the bones, the original and deformable inner surfaces of the soft tissues within the cut regions are first rigidly registered (potentially using manual landmarks), and then the distance between the surfaces is determined (Fig. 9). Table 2 reports the displacements of the cut bones in the experiments where the desired post-operative faces were specified as in Fig. 7b.

Table 2 The repositioning of the cut bones

Region	Reference axis/point	Displacements	Direction
Mid-face	Coronal	11 mm	Forward
Mid-face	Axial	5 mm	Downwards
Mid-face	Coronal/center	2.5°	Clockwise
Mid-face	Sagittal	2 mm	Right
Mid-face	Sagittal/center	5°	Clockwise

3.2 Performance evaluation

3.2.1 Experiment 1

Comparing the predicted data with the actual post-operative data is an effective way to measure the errors of the soft tissue model. First, we acquired the pre- and post-operative CT datasets of a patient (mid-face craniofacial dysostosis) who underwent mid-face distraction osteotogenesis using Le Fort III osteotomy. Then, a mixed volumetric mesh model containing all the facial tissues was generated as described in Section 2.2, having 10 873 prism elements for the skins and 110 475 tetrahedron elements for the internal soft tissues. Subsequently, the actual post-operative CT data was rigidly registered to the pre-operative CT data using the maximization of mutual information on an unaltered subvolume (Maes *et al.*, 1997). According to the registered results, the surface representation of the skin and skull was generated, and the cut regions of the bones were determined. Therefore the displacements of the different bone parts were calculated by mapping the surface representation to the mixed volumetric mesh of the soft tissue model, and thus the boundary conditions of the soft tissue model can be defined.

To prove the superiority of the mixed element model, some conventional methods consisting of a linear finite element model (LFEM) (Koch *et al.*, 1996), a mass tensor model (MTM) (Cotin *et al.*, 2000), and a non-linear finite element model (NFEM) were introduced to simulate the deformation of the soft tissues. During the simulation, all of these traditional models were based on the uniform tetrahedral elements and the C^0-continuous shape functions. We measured separately the distance errors between the predicted face and the actual post-operative face.

Fig. 10 shows the distance errors between the corresponding nodes of the predicted and the actual

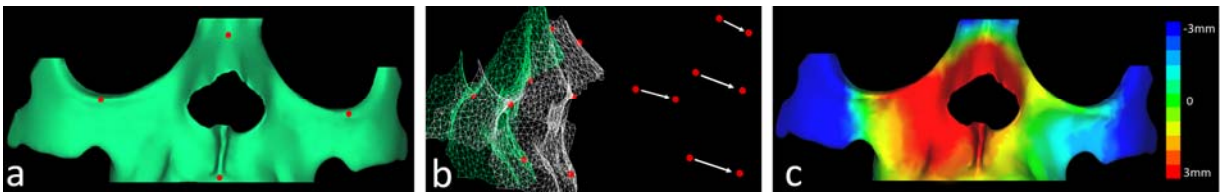

Fig. 9 The cut surface with four manual landmarks (a), the registration of the original and deformable cut surfaces of the soft tissues (b), and the distance map between the two surfaces (c)

facial surfaces. The distance errors were visualized by color coding. The statistical results of the average, the variance, and the maximum distance errors are reported in Table 3, showing that the mixed-element model obtained the most accurate result. The variance of the distance errors was the least in all methods, which means the mixed element model is the most stable. In addition, the average error was less than 1.0 mm and the maximum error stayed below 2.0 mm.

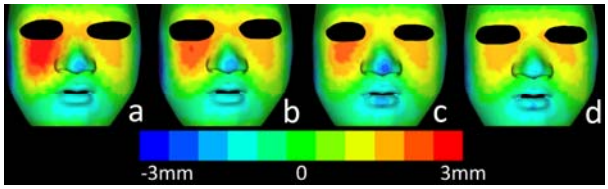

Fig. 10 Post-operative outline of the patient predicted by four different deformable models

Distance errors between corresponding points of the predicted and actual facial appearances are visualized by color coding. (a) Linear finite element model (LFEM); (b) Mass tensor model (MTM); (c) Non-linear finite element model (NFEM); (d) The proposed mixed element model (NFM-EM)

Table 3 The statistical results for four different computational models

Method	Distance error (mm)		
	Average	Variance	Maximum
LFEM	1.34	1.42	3.52
MTM	1.25	1.28	3.53
NFEM	1.17	1.25	2.43
NFM-EM	0.93	0.79	1.93

3.2.2 Experiment 2

Sub-experiment 1 (S1): The predicted facial surface in Experiment 1 is defined as the pre-specified target face. The soft tissue model has identical deformable regions to above. We compared the predicted results with the actual applied movements of the bones. Fig. 11a shows the distance map between the actual bone movements and the predicted results.

Sub-experiment 2 (S2): From the co-registered post-operative data in Experiment 1, a surface representation of the skin was generated, and it was defined as the pre-specified target face. In addition, the deformable regions of the soft tissue model were determined in terms of the cut surfaces of the pre-operative skull. Thus, the experiment can be implemented as described in Section 3.1. The predicted results were compared with the actual applied movements of the bones. The distance map between the actual bone movements and the predicted results was visualized by color coding (Fig. 11b).

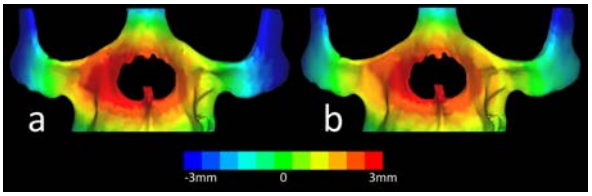

Fig. 11 Distance map between the actual bone movements and the predicted results visualized by color coding

(a) The predicted facial surface in Experiment 1 is defined as the pre-specified target face; (b) The surface representation of the skin of the post-operative data is defined as the pre-specified target face

Table 4 summarizes the outcome of the statistical analysis for the two sub-experiments S1 and S2, showing the average, the variance, and the maximum errors of the distance map between the predicted results and the actual applied movements. S1 and S2 nearly had the same errors (Table 4). These results show that the biomechanical model introduced minor errors in this simulation.

Table 4 The statistical results at various experiments using the mixed-element biomechanical model

Sub-experiment	Distance error (mm)		
	Average	Variance	Maximum
1	1.87	2.93	3.57
2	1.58	2.56	3.21

3.2.3 Experiment 3

To investigate more factors that affect the predicted results, the following quantitative protocol is defined to evaluate the experimental results:

1. After registration of the original and deformable inner surfaces of the soft tissues, the displacements of the cut bones are measured.

2. These results are used to define the boundary conditions for predicting the post-operative face, through application of the same biomechanical model used in Section 2 (details of the method for predicting the soft tissue deformation can be found in Mollemans *et al.* (2007)).

3. The performance quality is given by the distance map between the pre-specified and predicted facial outlines (which is simple to compute as they derive from the same mesh). The distance map can be visualized or statistically analyzed (Fig. 12). At the left of Fig. 12, three different target faces were pre-specified and the same cut regions were defined. In Figs. 12a and 12b, the pre-specified target faces were warped only within the cut regions. In Fig. 12c, the chin was also warped. The distance map was visualized by color coding over the facial surfaces. A negative error value means that the predicted skin surface lies behind the pre-specified skin surface.

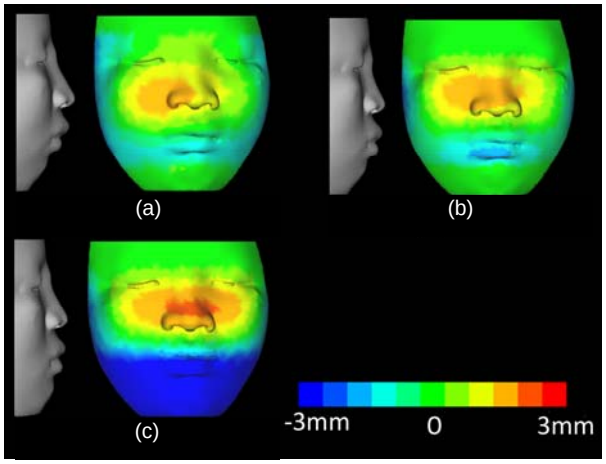

Fig. 12 Different simulation results for three different target faces at the same cut regions

In (a) and (b), the pre-specified target faces are warped only within the cut regions; in (c), the chin is also warped. The distance map between the pre-specified facial surfaces and the predicted faces based on the deformation of the soft tissues is visualized using color coding. A negative error value means that the predicted skin surface lies behind the pre-specified skin surface

In Figs. 12a and 12b, the average error within the cut regions was below 0.75 mm, with 90% of the nodal differences below 1.5 mm, showing that the accuracy of the simulation highly depends on the definition of the cut regions of the bones (osteotomies).

4 Discussion

In this paper, a novel approach was proposed to help surgeons automatically compute an optimal surgical plan by directly specifying the desired correction to a facial outline. This approach is effectively the inverse problem in predicting soft tissue deformation. The first step is to specify a desired outline using a 3D sculpturing tool. Then the displacements corresponding to the differences of node coordinates between the original and specified face meshes were used to drive the deformation of the facial soft tissues. After registering the deformable contact surfaces and the cut bone surfaces, the final positions of the cut bones are estimated.

The investigation shows that the errors derive from two aspects: the soft tissue simulation and the definition of the bone cuts (osteotomies). An accurate biomechanical model is the prerequisite to the implementation of this method. Therefore, in this work, non-linear finite mixed-element modeling was employed to simulate the deformation of the soft tissues. In this way, the different biomechanical characteristics of the skin and internal tissues were effectively incorporated into the soft tissue model of the face, enabling the potential for significantly higher accuracy in soft tissue simulation.

To further validate the accuracy of the algorithm, Experiment 1 was used to measure and evaluate the errors of the predicted results. The experimental results show that this method, as a mathematical algorithm, can provide enough accuracy to simulate the deformation of the soft tissues.

In addition, the predicted facial surface in Experiment 1 was defined as the pre-specified target face, and the movement of the bone fragments was estimated. Then in Experiment 2, we compared the predicted results with the actual applied movements, and quantitatively evaluated the errors. The average error was 1.87 mm and the variance error was 2.93 mm.

Experiment 3 shows that the performance highly depends on the consistency of the pre-specified facial profile and the cut regions. Therefore, pre-specifying a target face and defining the cut regions must be completed with the help of a surgeon.

In conclusion, the results show that the errors generated range from 0 to 3 mm. Furthermore, the real accuracy of this system is determined by the accuracy in Experiment 1 and Experiment 3, and the

errors will be 3 mm. However, since a planning accuracy of 0.5 mm is required, the advances in the accuracy of the system have to be done before this method can be successfully introduced in clinical practice.

The quantitative results also indicate that large deviations exist outside of the cut regions, with certain portions of the face (the lips and the nose) having consistently large differences due to the complicated boundary conditions in these regions.

Furthermore, the cranio-maxillofacial surgery involves some functional organs (e.g., the brain). Many problems need to be solved before applying it in the clinic practice. Therefore, surgeons still have to rely on their experiences to make a real plan. Of course, we will consider automated ways for defining the cut regions based on facial anatomy and desired post-operative facial appearances in the future work, to further improve the effectiveness of the prediction.

5 Conclusions

This work presents a novel method for automatic planning of bone-related procedures in craniofacial surgery. The approach estimates an optimal skull-remodeling scheme based on a pre-specified facial outline. Furthermore, an improved biomechanical model is proposed for soft tissue deformation, which better addresses the heterogeneity in geometry and material properties found in soft tissues of the face. In the quantitative evaluation and the comparison, the average errors and the variance are the least in all methods, which means the NFM-EM is the most stable model. In addition, we have demonstrated and validated this method in various experiments, and the results are highly promising with respect to clinical standards. Most importantly, the proposed paradigm is a fundamentally more natural and efficient way to optimize surgical planning.

Future work will expand on the evaluation studies, including the use of qualitative protocols (Westermark *et al*., 2005; Mollemans *et al*., 2007), and consider automated ways for defining the cut regions based on facial anatomy and desired post-operative facial appearances.

Acknowledgements

The authors would like to thank the anonymous reviewers for their comments and suggestions, which help improve the quality of this work greatly, and Prof. Xiong-zheng MU and Dr. Zhe-yuan YU with the Shanghai 9th People's Hospital for their assistance in acquiring patients dataset and validating the results.

References

Chabanas, M., Payan, Y., Marecaux, C., Swider, P., Boutault, F., 2004. Comparison of linear and non-linear soft tissue models with post-operative CT scan in maxillofacial surgery. *LNCS*, **3078**:19-27. [doi:10.1007/978-3-540-25968-8_3]

Cotin, S., Delingette, H., Ayache, N., 2000. A hybrid elastic model allowing real-time cutting, deformations and force-feedback for surgery training and simulation. *The Vis. Comput.*, **16**(8):437-452. [doi:10.1007/PL00007215]

Everett, P., Seldin, E.B., Troulis, M., Kaban, L.B., Kikinis, R., 2000. A 3D System for Planning and Simulating Minimally-Invasive Distraction Osteogenesis of the Facial Skeleton. *LNCS*, **1935**:1029-1039.

Fung, Y., 1993. Biomechanics: Mechanical Properties of Living Tissue. Springer, New York.

Gladilin, E., Zachow, S., Deuflhard, P., Hege, H.C., 2001. A Biomechanical Model for Soft Tissue Simulation in Craniofacial Surgery. Proc. Int. Workshop on Medical Imaging and Augmented Reality, p.137-141.

ITK-SNAP, 2009. Penn Image Computing and Science Laboratory (PICSL). University of Pennsylvania. Available from http://www.itksnap.org/ [Accessed on Nov. 18, 2009].

Keeve, E., Girod, S., Pfeifle, P., Girod, B., 1996. Anatomy-Based Facial Tissue Modeling Using the Finite Element Method. Proc. 7th Conf. on Visualization, p.21-28.

Keeve, E., Schaller, S., Girod, S., Girod, B., 1997. Adaptive surface data compression. *Signal Process.*, **59**(2):211-220. [doi:10.1016/S0165-1684(97)00047-9]

Koch, R.M., Gross, M.H., Carls, F.R., von Buren, D.F., Fankhauser, G., Parish, Y.I.H., 1996. Simulating Facial Surgery Using Finite Element Models. Proc. 23rd Annual Conf. on Computer Graphics and Interactive Techniques, p.421-428. [doi:10.1145/237170.237281]

Kvistedal, Y.A., Nielsen, P.M., 2004. Investigating Stress-Strain Properties of In-Vivo Human Skin Using Multiaxial Loading Experiments and Finite Element Modeling. Proc. 26th IEEE EMBS, p.5096-5099.

Lee, Y., Terzopoulos, D., Walters, K., 1995. Realistic Modeling for Facial Animation. Computer Graphics Proc., Annual Conf. Series, p.55-62.

Maes, F., Collignon, A., Vandermeulen, D., Marchal, G., Suetens, P., 1997. Multimodality image registration by

maximization of mutual information. *IEEE Trans. Med. Imag.*, **16**(2):187-198. [doi:10.1109/42.563664]

Mollemans, W., Schutyser, F., Nadjmi, N., Maes, F., Suetens, P., 2007. Predicting soft tissue deformations for a maxillo-facial surgery planning system: from computational strategies to a complete clinical validation. *Med. Image Anal.*, **11**(3):282-301. [doi:10.1016/j.media.2007.02.003]

Natali, A., Carniel, E., Pavan, P., Dario, P., Izzo, I., 2006. Hyperelastic Models for the Analysis of Soft Tissue Mechanics: Definition of Constitutive Parameters. First IEEE/RAS-EMBS Int. Conf. on Biomedical Robotics and Biomechatronics, p.188-191. [doi:10.1109/BIOROB.2006.1639082]

Paiva, A., Lopes, H., Lewiner, T., 2006. Robust Adaptive Meshes for Implicit Surfaces. IEEE Proc. 19th Brazilian Symp. on Computer Graphics and Image Processing, p.205-212. [doi:10.1109/SIBGRAPI.2006.40]

Picinbono, G., Delingette, H., Ayache, N., 2001. Non-linear and Anisotropic Elastic Soft Tissue Models for Medical Simulation. IEEE Int. Conf. on Robotics and Automation, p.1370-1375.

Picinbono, G., Delingette, H., Ayache, N., 2003. Non-linear anisotropic elasticity for real-time surgery simulation. *Graph. Models*, **65**(5):305-321. [doi:10.1016/S1524-0703(03)00045-6]

Schutyser, F., van Cleynenbreugel, J., Ferrant, M., Schoenaers, J., Suetens, P., 2000. Image-based 3D planning of maxillofacial distraction procedures including soft tissue implications. *LNCS*, **1935**:999-1007. [doi:10.1007/978-3-540-40899-4_104]

Sokhanvar, S., Dargahi, J., Packirisamy, M., 2008. Hyperelastic modeling and parametric study of soft tissue embedded lump for MIS applications. *Int. J. Med. Rob. Comput. Assist. Surg.*, **4**(3):232-241. [doi:10.1002/rcs.202]

Wang, S., Yang, J., 2009. An improved finite element model for craniofacial surgery simulation. *Int. J. Comput. Assist. Radiol. Surg.*, **4**(6):579-587. [doi:10.1007/s11548-009-0373-3]

Wang, S., Yang, J., 2010. Simulating cranio-maxillofacial surgery based on mixed-element biomechanical modeling. *Comput. Methods Biomech. Biomed. Eng.*, online. [doi:10.1080/10255840903317386]

Wang, S., Yang, J., Gee, J.C., 2010. Advances in collision detection and non-linear finite mixed element modelling for improved soft tissue simulation in craniomaxillofacial surgical planning. *Int. J. Med. Rob. Comput. Assist. Surg.*, **6**(1):28-41.

Westermark, A., Zachow, S., Eppley, B., 2005. Three-dimensional osteotomy planning in maxillofacial surgery including soft tissue prediction. *J. Craniofac. Surg.*, **16**(1):100-104. [doi:10.1097/00001665-200501000-00019]

Zachow, S., Gladiline, E., Hege, H.C., Deuflhard, P., 2000. Finite Element Simulation of Soft Tissue Deformation. Proc. 14th Int. Symp. on Computer Assisted Radiology and Surgery, p.23-28.

Zachow, S., Hierl, T., Erdmann, B., 2004. A Quantitative Evaluation of 3D Soft Tissue Prediction in Maxillofacial Surgery Planning. Proc. 3rd Jahrestagung der Deautschen Gesellschaft fur Computer- und Robotor-Assistierte Chirurgie, p.75-79.

Zachow, S., Hege, H.C., Deuflhard, P., 2006. Computer-assisted planning in cranio-maxillofacial surgery. *J. Comput. Inform. Technol.*, **14**(1):53-64. [doi:10.2498/cit.2006.01.06]